THE JOURNAL OF BIOLOGICAL CHEMISTRY Vol. 278, No. 30, Issue of July 25, pp. 27464–27472, 2003

Printed in U.S.A.

Structural Flexibility of Multifunctional HABP1 May Be Important for Regulating Its Binding to Different Ligands*

Received for publication, July 6, 2002, and in revised form, April 8, 2003
Published, JBC Papers in Press, April 27, 2003, DOI 10.1074/jbc.M206696200

Babal Kant Jha‡, Dinakar M. Salunke§, and Kasturi Datta‡¶‖

From the ‡Biochemistry Laboratory, School of Environmental Sciences, Jawaharlal Nehru University, §Structural Biology Unit, National Institute of Immunology, Aruna Asaf Ali Marg, and ¶Special Center for Molecular Medicine, Jawaharlal Nehru University, New Delhi 110067, India

Hyaluronan-binding protein 1 (HABP1)/p32/gC1qR was characterized as a highly acidic and oligomeric protein, which binds to different ligands like hyaluronan, C1q, and mannosylated albumin. It exists as trimer in high ionic and reducing conditions as shown by crystal structure. In the present study, we have examined the structural changes of HABP1 under a wide range of ionic environments. HABP1 exhibits structural plasticity, which is influenced by the ionic environment under *in vitro* conditions near physiological pH. At low ionic strength HABP1 exists in a highly expanded and loosely held trimeric structure, similar to that of the molten globule-like state, whereas the presence of salt stabilizes the trimeric structure in a more compact fashion. It is likely that the combination of the high net charge asymmetrically distributed along the faces of the molecule and the relatively low intrinsic hydrophobicity of HABP1 result in its expanded structure at neutral pH. Thus, the addition of counter ions in the molecular environment minimizes the intramolecular electrostatic repulsion in HABP1 leading to its stable and compact conformations, which reflect in its differential binding toward different ligands. Whereas the binding of HABP1 toward HA is enhanced on increasing the ionic strength, no significant effect was observed with the two other ligands, C1q and mannosylated albumin. Thus, although HA interacts only with compact HABP1, C1q and mannosylated albumin can bind to loosely held oligomeric HABP1 as well. In other words, structural changes in HABP1 mediated by changes in the ionic environment are responsible for recognizing different ligands.

The ubiquitous glycosaminoglycan hyaluronan is an unbranched polysaccharide composed entirely of a repeating disaccharide, D-glucuronic acid (β1→3) *N*-acetyl-D-glucosamine (β1→4), which, unlike other glycosaminoglycans, is neither attached to a protein core nor *O*- or *N*-sulfated. It has diverse biological roles in vertebrates; these include acting as a vital structural component of connective tissues; the formation of loose hydrated matrices that allow cells to divide and migrate during development, immune cell adhesion, and activation; and in intracellular signaling (1–5). This wide range of activities in fact results from its interactions with a large number of proteins termed as hyaladherin that exhibit significant differences in their tissue expression, cellular localization, specificity, affinity, and regulation (2).

Hyaluronan-binding protein 1 (HABP1)[1] one of the members of hyaladherin family, is originally purified as a novel receptor of hyaluronan by our group (6–8). We established its role in cell adhesion and tumor invasion (8–9) and sperm maturation and motility (10, 11). The cDNA encoding hyaluronan-binding protein 1 has been cloned by immunoscreening the human skin fibroblast expression library, sequenced, and overexpressed (7). Sequence analysis confirmed that although HABP1 is synthesized as pro-protein form of 282 amino acids, the first 73 NH_2-terminal residues are cleaved immediately to generate a mature form of HABP1. The presence of an HA-binding motif has been confirmed, and subsequently the recombinant protein has been shown to bind HA. The multifunctional nature of HABP1 is revealed due to its sequence identity with p32, a protein co-purified with splicing factor SF2 (12) and with the receptor of globular head of complement factor 1q (gC1qR) (13) and is represented as synonyms of C1QBP, gC1qR, and p32 (GenBank™ accession number NP_001203). Many homologous and identical genes of this molecule have been identified in eukaryotic species, ranging from fungi to mammals from sequence analysis data as well as biochemical studies (14). This protein is reported by several investigators (15–16) to be present in cytosol, mitochondria, and cell surface in different cell types. Even its presence in the nucleus of virally transformed cell lines is demonstrated. This is probably explained as the role of HABP1 in cellular signaling is well documented and has been strengthened by our recent observations that being an endogenous substrate of ERK1/ERK2, it translocated to nucleus upon phosphorylation (17).

The crystal structure of HABP1 showed that it exists as a homotrimer, and each protomer consists of seven consecutive twisted anti-parallel β-sheets flanked by one NH_2-terminal and two COOH-terminal α-helices and that the terminal α-helices have extensive intra- as well as intermolecular contacts. It has been postulated that these terminal helices are critical for maintaining the trimeric assembly and protein-protein interactions (14). Among these structural arrangements, the HA-binding motif in each trimeric assembly is solvent-exposed. In our previous report (18), we have shown that HABP1 exists predominantly as a non-covalently linked trimer near physiological conditions and as a hexamer (dimer of trimers) in the

* This work was supported in part by Grants from Department of Biotechnology and Science & Technology, Government of India. The costs of publication of this article were defrayed in part by the payment of page charges. This article must therefore be hereby marked "*advertisement*" in accordance with 18 U.S.C. Section 1734 solely to indicate this fact.

‖ To whom correspondence should be addressed: 103, Biochemistry Laboratory, SES, Jawaharlal Nehru University, New Delhi 110067, India. Tel.: 91-11-26704327; Fax: 91-11-26172438 or 26165886; E-mail: kdatta@mail.jnu.ac.in and datta_k@hotmail.com.

[1] The abbreviations used are: HABP1, hyaluronan-binding protein 1; ANS, 1-anilinonaphthalene-8-sulfonate; AN, anilinonaphthyl; ANM, *N*-(1-anilinonaphthyl-4)maleimide; HA, hyaluronan; DMA, D-mannosylated albumin; ABTS, 2,2′-azinobis(3-ethylbenzothiazoline-6-sulfonic acid); FRET, fluorescence resonance energy transfer.

oxidative environment. The isoelectric point (pI) of HABP1 is 4.10, and there are more than average polar amino acid residues (43%) present in the molecule. In addition, asymmetric charge distribution on the surface of HABP1 allows the predominance of electrostatic interactions in dictating its folding topology and tertiary interactions.

The relative role of the contribution of electrostatic interactions to protein stability, compared with that of hydrophobic interactions, has been the subject of long-standing queries (19). In the present study, we examine the physical stability, structural flexibility, and conformational diversity of HABP1 under *in vitro* conditions as a function of ionic strength to provide a rationale for the marginal stability at neutral pH and to explain its differential binding toward ligands.

EXPERIMENTAL PROCEDURES

Materials—EAH-Sepharose 4B, Superose-6 column, and low molecular weight markers were obtained from Amersham Biosciences. All other chemicals (unless otherwise mentioned) were obtained from Sigma. For every purpose MilliQ™ grade water was used.

Purification and Estimation of HABP and Preparation of Its Polyclonal Antibodies—Recombinant HABP1 (amino acids 74–282, with Leu^{74} to Met^{74} substitution) was overexpressed in *Escherichia coli* as described earlier (7). HABP1 was purified by a 65–90% ammonium sulfate cut, followed by ion exchange chromatography on MonoQ™ HR 10/10 column (Amersham Biosciences), interfaced with an FPLC™ system (Amersham Biosciences) using a linear gradient of 0–1 M NaCl in 20 mM HEPES, 1 mM EDTA, 1 mM EGTA, 5% glycerol, and 0.2% 2-mercaptoehanol, pH 7.5, followed by hyaluronan-Sepharose affinity column chromatography with the modification of an earlier report (18). Affinity-purified HABP1 was further purified by size exclusion chromatography in 10 mM phosphate-buffered saline containing 150 mM NaCl and 0.2% 2-mercaptoethanol. The antibodies against the purified recombinant HABP1 were raised in New Zealand White rabbit as reported earlier (7).

For all practical purposes the concentration of a known aliquot was determined in 20 mM phosphate buffer, pH 6.5, containing 6 M guanidinium HCl by measuring the absorbance at 280 nm at 25 °C on a Cary100 Bio UV-visible double beam spectrophotometer (Varian Inc., Australia) interfaced with peltier thermal controller. The molar extinction coefficient of denatured HABP1 was calculated by the method reported earlier (20) and was found to be 22,190 at 280 nm, which corresponds to $A^{0.1\%} = 0.932$.

Gel Permeation Chromatography—Gel permeation chromatography of HABP1 was carried out on Superose 6™ (1 × 30 cm) analytical column (Amersham Biosciences) interfaced with an FPLC™ system in 10 mM phosphate buffer, containing 0.1% 2-mercaptoethanol (v/v) and varying concentrations of either NaCl or KCl, pH 7.2, at a flow rate of 0.3 ml/min. Typically 100 μl of 1 mg/ml HABP1 in desired buffer was injected in each case. The standard molecular weight markers of known molecular weight and Stokes radius, *e.g.* alcohol dehydrogenase (150 kDa, 46 Å), bovine serum albumin (67 kDa, 35.5 Å), ovalbumin (43 kDa, 30.5 Å), chymotrypsinogen (25 kDa, 20.9 Å), and ribonuclease A (13.7 kDa, 16.4 Å), were independently run in different cases before and after each run. Calculation of Stokes radius was done by the method reported earlier (21, 22).

Covalent Cross-linking of HABP1 Subunits—To HABP1 (0.2 μM) in 10 mM phosphate buffer, pH 7.2, containing varying amounts of NaCl (0–1 M), an aliquot of 25% (mass/volume) glutaraldehyde was added so as to make a final concentration ranging from 1 to 4% of glutaraldehyde. This sample was incubated at 25 °C for 10 min followed by quenching of the cross-linking reaction by adding 30 mM of 2-mercaptoethanol (23). After 20 min of incubation sodium deoxycholate stock was added to the reaction mixture to a final concentration of 0.3% (w/v). The pH of the reaction mixture (in 10 mM phosphate buffer containing varying amounts of NaCl, pH 7.2) was lowered to 2.0–2.5 by addition of concentrated orthophosphoric acid that resulted in the co-precipitation of cross-linked HABP1 with sodium deoxycholate. After centrifugation (13,000 × *g*, 4 °C) the precipitate was re-dissolved in 0.1 M Tris/HCl, pH 8.0, 1% SDS, and 0.1% 2-mercaptoethanol and heated at 90–100 °C for 3 min in a water bath and analyzed by electrophoresis.

ANS Binding Assay—The ANS binding assay was performed as reported earlier (24). Briefly, the reagent 1-anilinonaphthalene-8-sulfonate (ANS), dissolved in water, was added to the protein samples, in 10 mM phosphate buffer containing different amounts of NaCl, to a final concentration of 5 μM and incubated for 10 min at room temperature in each case. ANS added samples of HABP1 were excited at 380 nm, and the emission spectra were recorded from 390 to 690 nm.

Circular Dichroism Spectral Studies—All of the far-UV CD spectra of HABP1 were recorded on a Jasco 715 spectropolarimeter in 10 mM phosphate buffer containing different amounts of NaCl to achieve the desired ionic strength from 250 to 190 nm at 10 °C. The samples were prepared 4 h before recording the spectra in desired buffer and centrifuged for 20 min at 10,000 × *g* prior to recording. A rectangular cuvette of 2 mm path length was used throughout the experiment. The concentration of protein was kept constant at 10 μM. Data were recorded at a scan speed of 50 nm/min with a response time of 1 s at a bandwidth of 1 nm, and data were accumulated at 0.1-nm step intervals. The buffer base line was subtracted in each case. Estimation of secondary structural content was performed using the software supplied with the instrument.

Fluorescence Measurement—All of the fluorescence measurements were carried out on a Cary Eclipse™ spectrofluorimeter (Varian Inc. Australia) at 25 °C. The concentration of the protein (0.05 mg/ml) was chosen so that the absorbance at 280 nm was always ≤0.1 to avoid any inner filter effect. Prior to every run, buffers and samples were either filtered through 0.22-μ Millipore membranes or centrifuged at 10,000 × *g* at 4 °C for 15 min. The path length of 1 cm, excitation and emission slit width of 2.5 and 5 nm, respectively, and photomultiplier voltage of 600 V were kept constant for all the fluorescence measurements. The base-line correction was done with buffer alone prior to every run. For intrinsic fluorescence measurements, samples containing same amount of protein and varying amounts of NaCl were excited at 282 nm, and the emission was recorded at 350 nm.

Iodide Quenching—0.05 mg/ml HABP1 in 10 mM phosphate buffer with varying amounts of NaCl were incubated with 0–0.2 M potassium iodide in the presence of 10 μM sodium thiosulfate for 1 h at 25 °C, excited at 295 nm, and the emission was recorded at 350 nm, and the emission intensity was plotted against the quencher concentration.

N-(1-Anilinonaphthyl-4)maleimide (ANM) Labeling of HABP1 and Its Fluorescence Measurement—*N*-(1-Anilinonaphthyl-4)maleimide was covalently attached to the only cysteine (Cys^{186}) present in HABP1 by using the method of Ohyashiki *et al.* (25) with slight modifications. Briefly, 1 mg/ml HABP1 in 10 mM phosphate buffer was treated with 10 mM dithiothreitol and dialyzed extensively against 10 mM Tris/H_2SO_4 buffer, pH 7.2, containing 50 μM dithiothreitol. To this solution, 1 mM of final concentration of ANM, dissolved in trace amount of acetone, was added and incubated for 60 min at 25 °C. The reaction was stopped by adding 10 mM of dithiothreitol and dialyzed against 10 mM phosphate buffer containing different amounts of NaCl. The number of anilinonaphthyl (AN) group was determined spectrophotometrically with a millimolar extinction coefficient of 10.8 mM^{-1} cm^{-1} at 345 nm (24). The labeling is found to be 0.96 mol of AN group per mol of HABP1 monomer (considering the sequence-derived molecular mass of 23,801.1 Da for HABP1). For monitoring the conformational change associated around Cys^{186} the samples were excited at 350 nm, and the emission was recorded at 460 nm. To examine the resonance energy transfer, samples were excited at 295 nm, and the emission spectra were recorded from 310 to 510 nm with different amounts of NaCl added to 10 mM phosphate buffer, pH 7.2. Base-line correction was done with the buffer alone in each case.

Limited Proteolysis—HABP1 (1 μM) in 10 mM sodium phosphate buffer, pH 7.2, was incubated with varying amounts of NaCl to achieve the desired ionic strength for 2 h at 25 °C followed by incubation with trypsin (protease/HABP1 ratio 1:100 w/w) for 2 h at 25 °C in a 200-μl reaction volume. At higher salt concentrations the protease enzyme ratio was increased so as to compensate for the loss of enzyme activity as a result of the increase in ionic strength as described earlier (26). The proteolysis was stopped using soybean trypsin inhibitor (Invitrogen) by adding 1:2 w/w enzyme inhibitor ratio (26). 200 μl of this digest was injected in high resolution Sephacryl S200™ (16:60) pre-packed column interfaced with AKTA™ Basic (Amersham Biosciences) pre-equilibrated with 10 mM phosphate buffer containing 150 mM of NaCl at a elution rate of 0.8 ml/min. The elution was monitored at 225 nm.

Ligand Binding Assays—Microtiter plate-binding assays were carried out to investigate the effect of ionic strength on the interactions of HA, DMA, and C1q with HABP1. The assays, which are based on those described previously (27–28), determine colorimetrically the level of binding of HABP1 to wells coated with HA, c1q, or DMA. All dilutions and incubations were performed in standard assay buffer (SAB, 10 mM phosphate buffer, pH 7.2) containing varying amounts of NaCl to achieve the desired ionic strength at room temperature. All washes

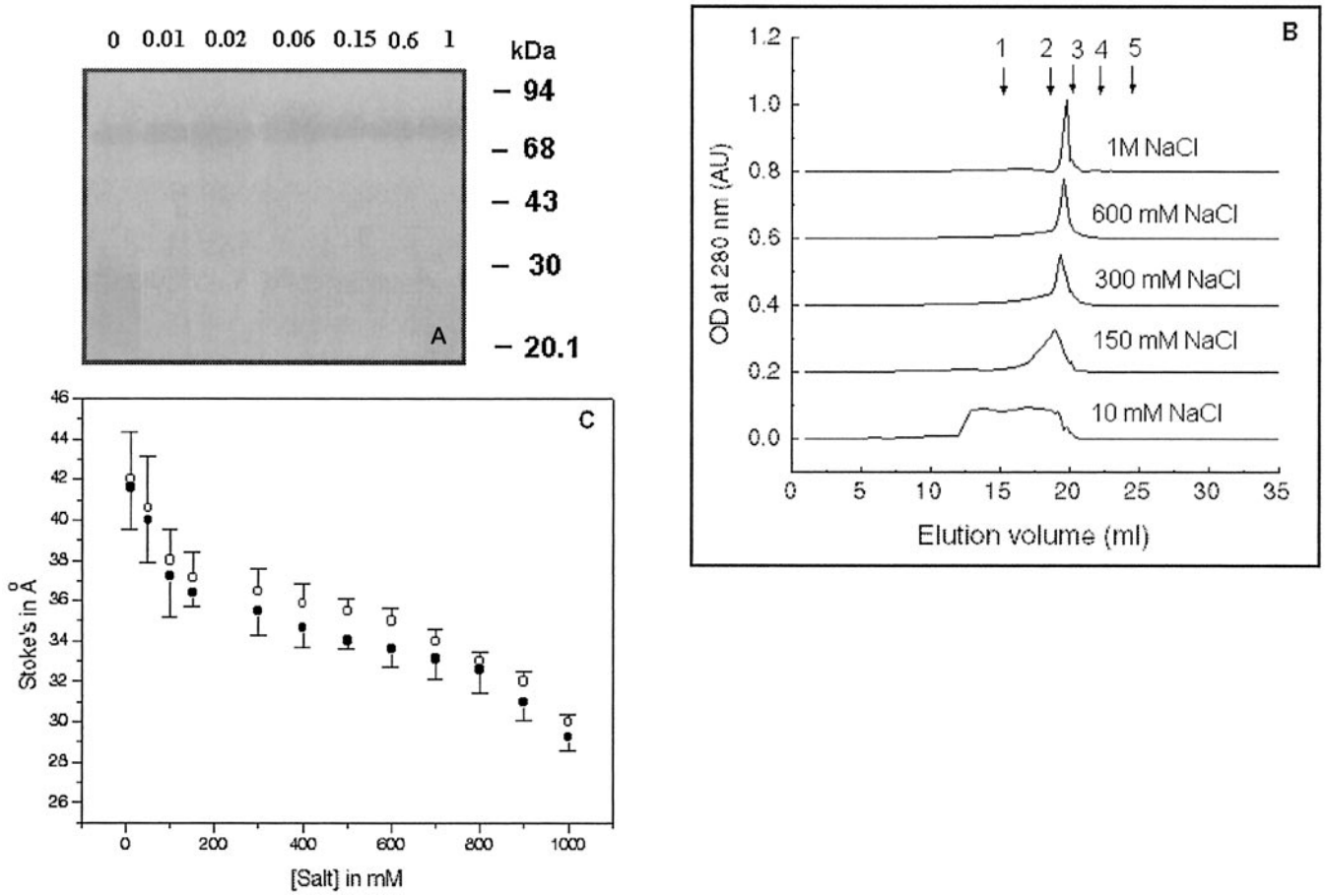

FIG. 1. **Salt-induced changes in hydrodynamic properties of trimeric HABP1.** *A*, covalent cross-linking of HABP1 subunit using 2% glutaraldehyde. 0.1 mg/ml HABP1 in 10 mM phosphate buffer, pH 7.2, incubated with different amounts of NaCl, shown on the *top* of the lane, was cross-linked using glutaraldehyde as described under "Experimental Procedures" and separated on 12.5% SDS-PAGE and stained with Coomassie Brilliant Blue R-250. Molecular mass markers are shown on the *right margin*. *B*, size exclusion chromatographic profiles of HABP1. 100 μl of 1 mg/ml HABP1 in 10 mM phosphate, pH 7.2, at different ionic strengths were injected on Superose 6 HR30 analytical column at an elution speed of 0.3 ml/min, and absorbance at 280 nm was plotted against elution volume. The ionic strength was achieved by adding required amount of NaCl to keep the molarity of phosphate and pH constant. The mean elution volumes of standard molecular mass markers of different Stokes radii are as follows: *arrow 1*, alcohol dehydrogenase (150 kDa, 46 Å); *arrow 2*, bovine serum albumin (67 kDa, 35.5 Å); *arrow 3*, ovalbumin (43 kDa, 30.5 Å); *arrow 4*, chymotrypsinogen (25 kDa, 20.9 Å); and *arrow 5*, ribonuclease A (13.7 kDa, 16.4 Å). The base line is translated upward for the clarity of data. *C*, hydrodynamic radius of HABP1. The change in the Stokes radius with increasing NaCl (*open circle*) and KCl (*solid circle*) concentration, calculated by taking the mean elution volume of each peak as described under "Experimental Procedures" and plotted against the ionic strength of the buffer. The standard deviation ($n = 3$) is shown as (±) *error bars* on each data point.

were performed in SAB containing 150 mM NaCl and 0.05% (v/v) Tween 20. Plastic Costar flat bottomed and high binding microtiter plates (EIA/RIA) were coated (in triplicate) overnight with 100 μl/well of 10 μg/ml HA and DMA, prepared as described earlier (29), and c1q in 20 mM carbonate buffer (Na_2CO_3-$NaHCO_3$), pH 9.6, at 4 °C. Control wells were treated with buffer alone. The coating solution was removed, and the plates were washed three times, and nonspecific binding sites were blocked by incubation with 1.5% (w/v) bovine serum albumin for 90 min at 37 °C, followed by three washes. Finally, the respective wells were rinsed three times with SAB containing different amounts of salt. 100 μl of 50 μg/ml HABP1 in 10 mM sodium phosphate buffer containing different amounts of NaCl was added to each well and incubated for 4 h at room temperature or overnight at 4 °C. Plates were washed three times, and 100 μl of a 1:5000 dilution of polyclonal anti-HABP1 antibodies (in SAB) was added and incubated for 90 min, followed by five washes. 100 μl/well of a 1:30,000 dilution of horseradish peroxidase-conjugated goat anti-rabbit IgG in SAB was added to each well and incubated for 1 h at room temperature. The secondary antibodies were sipped out of the wells and washed five times and finally rinsed with substrate buffer (100 mM phosphate-citrate buffer, pH 5.0). 100 μl of 0.6 mg/ml solution of 2,2′-azinobis(3-ethylbenzothiazoline-6-sulfonic acid) (ABTS) in substrate buffer containing 3 μl of H_2O_2/ml of buffer was added to each well and incubated for 10 min at 37 °C for color development. For competitive binding assays, 100 μl/well of 10 μg/ml of DMA was coated on microtiter plates and incubated with 100 μl of 1 μg/ml of biotinylated HABP1 in 10 mM phosphate buffer containing different amounts of salt, pH 7.2, which was preincubated with varying amounts of unlabeled HA, DMA, or C1q. The bound HABP1 was detected by 1:30,000 dilution of ExtrAvidin-horseradish peroxidase conjugate using ABTS as a substrate. Absorbance at 405 nm was determined on a microtiter plate reader (Bio-Rad model 550 microplate reader). All absorbances were corrected against blank wells. Each data point is the average of three similar sets of experiments. For absolute binding absorbance at 405 nm was plotted against the increasing salt concentrations, and for competitive binding assays the percentage inhibition was plotted against increasing concentrations of unlabeled ligands at different salt concentrations.

RESULTS

Decreased Hydrodynamic Volume of Trimeric HABP1 with Increasing Ionic Strength—In order to identify the oligomeric state of the molecule under the reducing conditions as a function of salt, covalent cross-linking of the oligomeric subunit was performed under the conditions of different ionic strength used throughout the experiment. The peak fractions of the protein eluted as a function of ionic strength on Superose 6 HR 10/30 column were cross-linked using 2% glutaraldehyde and examined on SDS-PAGE (Fig. 1*A*). The data showed that HABP1 exists predominantly as trimer in equilibrium with a small proportion of monomer in the absence of salt (Fig. 1*A*). The relative band intensities of the cross-linked product in the absence of salt indicate that this equilibrium is biased in the

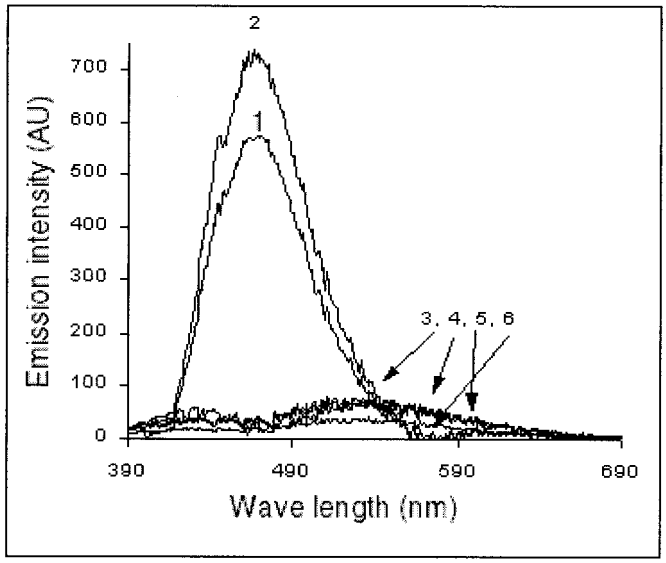

FIG. 2. **Existence of molten globule-like state of HABP1 at low ionic strength.** 0.05 mg/ml HABP1 in 10 mM phosphate buffer, pH 7.2, containing different amounts of NaCl at 25 °C was treated with a 5 μM final concentration of ANS and excited at 380 nm, and the emission spectra were recorded. The various curves represent the emission spectra in the presence of various amount of salt: 0 (*curve 1*), 20 (*curve 2*), 50 (*curve 3*), 150 (*curve 4*), 300 (*curve 5*), and 600 mM (*curve 6*). Blank (buffer alone) was run separately in each case and subtracted from the sample spectra under similar conditions.

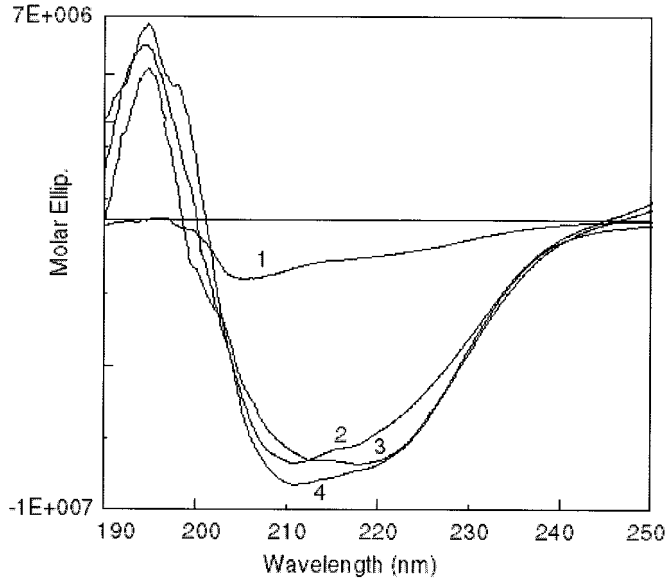

FIG. 3. **Effect of ionic strength on secondary structure of HABP1.** Far-UV CD spectra of HABP1 (10 μM) in 10 mM sodium phosphate buffer containing different amounts of salt. The various curves are the CD spectra of HABP1 in 0 (*curve 1*), 150 (*curve 2*), and 600 mM (*curve 3*), and 1 M (*curve 4*) of NaCl concentration.

favor of trimer. However, this protein exists only as a trimer in the presence of salt as low as 10 mM.

In order to examine if electrostatic repulsion in HABP1, an acidic protein, is indeed responsible for expanded structure in low ionic environment, size exclusion chromatography was carried out in 10 mM phosphate buffer, pH 7.2, containing 0.1% 2-mercaptoethanol with varying concentrations of NaCl 0.01–1 M (Fig. 1*B*). The elution peak at low ionic strength (0.01 M) is broad and diffused as against the peaks at higher ionic strengths, which are relatively sharp. The broad diffused nature of the peak under low ionic strength is perhaps due to the interactions of the gel filtration medium with the conformational ensemble of HABP1 that includes variations from the crystallographically observed compact structure. A gradual increase in elution volume (V_e) was observed with increasing salt concentrations, which reflects a gradual decrease in the hydrodynamic volume (V_h) of the molecule. Therefore size exclusion chromatographic data were further analyzed for calculating the hydrodynamic size of the molecule by comparing with the standard molecular weight markers of known Stokes radii as described earlier and plotted against the ionic strength (Fig. 1*C*, *open circles*). To see any cation specificity, a similar set of experiments was carried out in the presence of KCl, and the Stokes radius was plotted against the increasing concentration as shown in Fig. 1*C* (*solid circles*). The changes in cation-induced structural compaction did not suggest any specific ion selectivity. The important observations of our study are concerned with strikingly different state of compactness, induced by increasing amounts of salt in the molecular environment. For example, the loosely held trimers in the absence of salt were so expanded that they eluted much earlier than the compact trimer under the conditions involving 150 mM to 1 M NaCl/KCl. As the ionic strength is increased, there is a gradual increase in the compactness of trimer such that the compact form of the trimer has a Stokes radius of 36.9 Å at 150 mM and 31 Å at 1 M salt concentration (Fig. 1*C*) as compared with the most expanded trimer, which has a Stokes radii of 42 Å. Therefore, the broad peak corresponding to a Stokes radius of nearly 42 Å is apparently not due to any higher order oligomer because the whole experiment is conducted under reducing conditions, and the subsequent cross-linking experiment failed to identify any higher oligomer. To assess further the oligomeric distribution of HABP1 at higher salt concentrations, cross-linking as a function of glutaraldehyde was performed, and no detectable oligomer other than trimer was observed until 4% of glutaraldehyde at these salt concentrations (data not shown). Thus our results suggest that HABP1 exists as a loosely held expanded trimer in low ionic environments, which undergoes structural compaction with increasing ionic strength.

Existence of Expanded Trimeric HABP1 as a Molten Globule-like State in Low Ionic Environment—The presence of an expanded structure of trimeric HABP1 may result in the exposure of the hydrophobic core similar to the molten globule-like state of the molecule, if any. To investigate any such possibility in the case of HABP1, hydrophobic reporter dye, 1,10-anilinonaphthylsulfonate, binding was carried out at different ionic strengths. ANS is a weak fluorescent molecule when free. However, the fluorescence emission intensity increases with a characteristic blue shift in emission maximum when it is bound to the hydrophobic core of the protein (24). ANS binding was observed from enhancement of the emission intensity with a blue shift of nearly 50 nm with respect to free ANS under low ionic strength where protein exists predominantly as a loosely held trimer in dynamic equilibrium with a very small proportion of monomer (Fig. 2). Our observations on the significant increase of ANS binding suggests that the expanded trimer is somewhat similar to a molten globule-like state under low ionic environments. With an increase in ionic strength HABP1 folds appropriately into a stable conformation so that the hydrophobic core is inaccessible for ANS binding.

Effect of Ionic Strength on the Structural Properties of HABP1—To probe the ionic environment-mediated structural changes of HABP1 from expanded molten globule-like state to a compact stable folded form, spectroscopic investigations (far-UV CD, intrinsic as well as extrinsic fluorescence, fluorescence quenching, and fluorescence resonance energy transfer experiments) were carried out as a function of ionic strength.

To probe the structural changes in trimeric HABP1 as a

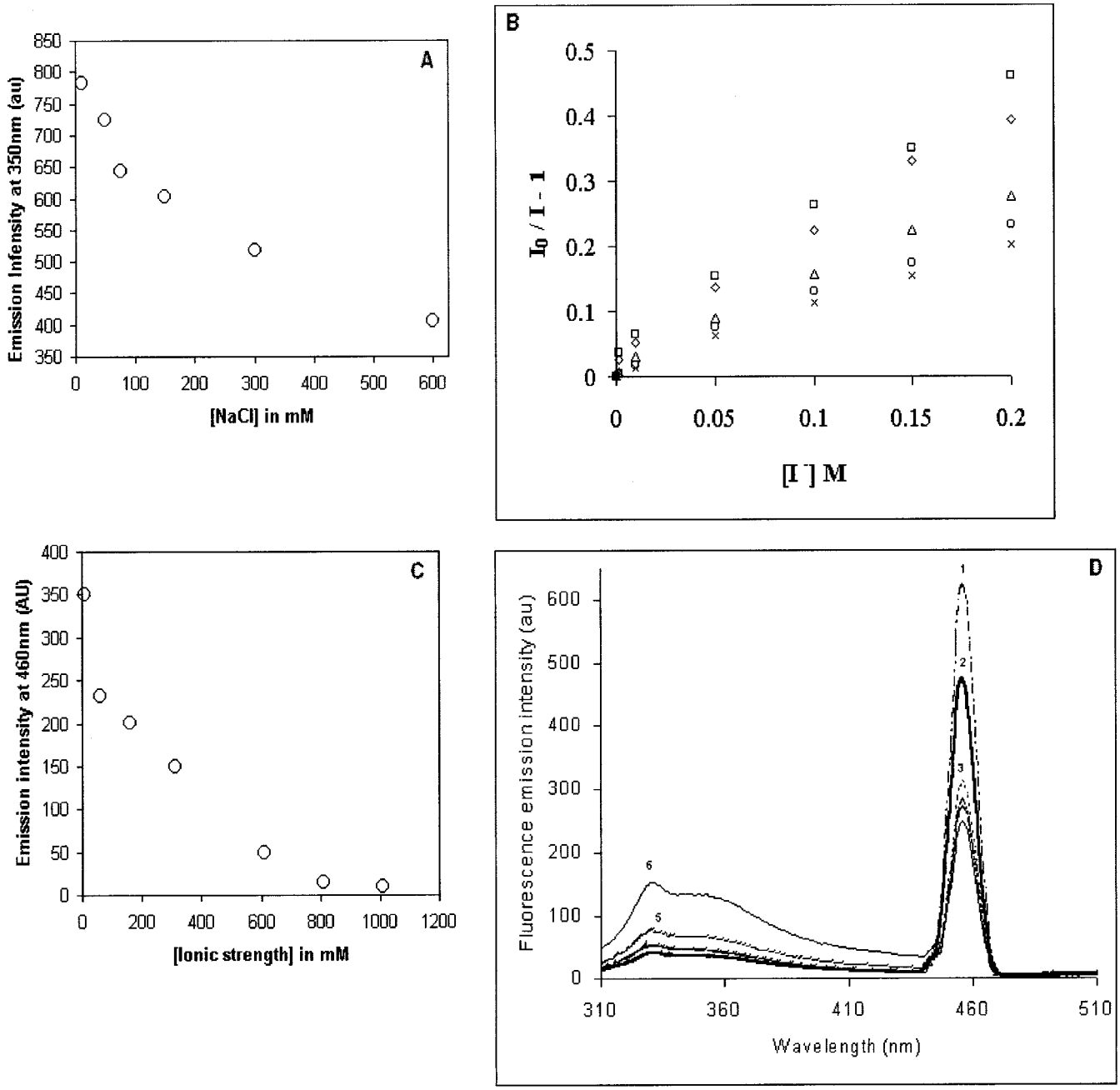

FIG. 4. **Salt-induced conformational change in HABP1.** *A*, intrinsic fluorescence measurement HABP1 (0.05 mg/ml) in 10 mM phosphate buffer, pH 7.2, at different ionic strength were excited at 282 nm, and emissions were recorded at 350 nm, blanks (buffer alone) were recorded prior to sample recording and subtracted from the sample and plotted against the salt concentration. *B*, iodide quenching of intrinsic fluorescence. 0.05 mg/ml of HABP1 was treated with different amounts (0–0.2 M) of KI with 10 μM sodium thiosulfate in 10 mM phosphate buffer containing the following: □, 10; ◇, 50; Δ, 150; ○, 600; and × 1000 mM of NaCl and excited at 295 nm. The emission was recorded at 350 nm. Emission intensity in the absence of KI is taken to be I_0 in each case and $I_0/I - 1$ was plotted against quencher concentration. *C*, extrinsic fluorescence measurements. The only cysteine in each HABP1 molecule was covalently tagged with *N*-(1-Anilinonaphthyl-4)maleimide as described under "Experimental Procedures" and excited at 350 nm, and emission was recorded at 460 nm. The change in fluorescence emission intensity of ANM-tagged cysteine was plotted against increasing salt concentrations. *D*, change in average distance between cysteine (Cys^{186}) and tryptophans in HABP1. The only cysteine (Cys^{186}) present in HABP1 was covalently tagged with *N*-(1-Anilinonaphthyl-4)maleimide (ANM), and 0.05 mg/ml of the modified protein in 10 mM phosphate buffer containing 1 M (*curve 1*), and 600 (*curve 2*), 300 (*curve 3*), 150 (*curve 4*), and 50 mM (*curve 5*) and in the absence of salt (*curve 6*) were excited at 295 nm, and emission were recorded from 310 to 510 nm.

function of ionic strength, its secondary structural content was investigated by far-UV circular dichroism spectroscopy. The spectra were recorded in 10 mM phosphate buffer, pH 7.2, at different ionic strength conditions using sodium chloride (0–1 M) and are presented in Fig. 3 after subtracting the buffer base line. The minima in the absence of salt lies at 205 nm, although it gives a double minima at 219.3 and 210 nm at higher salt concentrations (150 mM to 1 M, *curves 2–4*, Fig. 3) with nearly four times increase in molar ellipticity, indicating a shift toward more rigid and ordered structure. The secondary structural content of the molecule increases with increasing salt concentrations. Moreover, the percentage compositions of various secondary structural elements derived from our data under 600 mM of salt are in fair agreement with the crystal structure determined under almost similar conditions. However, in the absence of salt or at very low salt concentrations, the molecule tends to show loss in secondary structure.

In order to examine further the effect of ionic strength on the

local structure around tryptophan and cysteine in HABP1, intrinsic as well as extrinsic fluorescence and fluorescence resonance energy transfer experiments were carried out under different conditions of ionic strength.

HABP1 has three Trp residues spread all over the molecule (Trp^{109}, Trp^{219}, and Trp^{233}) with almost symmetrical microenvironment as calculated from the crystal structure. Intrinsic fluorescence studies were carried out to probe the relative change in fluorescence emission intensity as a function of increasing salt concentration. Samples were excited at 282 nm, and the emission was recorded at 350 nm. A gradual decrease in the tryptophan intensity was observed at 350 nm (Fig. 4*A*). The data suggest that the solvent accessibility of the three tryptophans together is reduced due to salt-induced structural compactness.

The exposure of tryptophan was also investigated by iodide quenching studies as described under "Experimental Procedures." Fluorescence emission intensities were corrected for any dilution effects and for iodide absorbance (if any) at the excitation wavelength. Fluorescence quenching data were analyzed according to the general form of the Stern-Volmer Equation 1 (30),

$$I_0/I = (1 + K_{SV}[Q]) \quad \text{(Eq. 1)}$$

where I_0 and I are the fluorescence intensities in the absence and presence of quencher, respectively; K_{SV} is Stern-Volmer quenching constant, and [*Q*] is the total quencher concentration. The data on the gradual decrease in K_{SV} with increasing salt concentrations support the intrinsic fluorescence studies on gradual inaccessibility of tryptophan residues to the solvent with increasing salt concentrations (Fig. 4*B*).

To assess further whether the local structural changes are indeed real, an extrinsic probe ANM was covalently attached to the only cysteine (Cys^{186}) present in each HABP1 molecule and was confirmed by spectrophotometry as described under "Experimental Procedures." It has been reported earlier that free ANM is non-fluorescent but becomes fluorescent when covalently attached to cysteine (24). The emission intensity of the AN group depends on the microenvironment around it. To investigate the solvent exposure of cysteine as a function of salt concentration, the AN group tagged HABP1 was excited at 350 nm, and the fluorescence emission intensity was recorded at 460 nm. The change in emission intensity as a function of salt was plotted and is presented in Fig. 4*C*. Interestingly, a gradual decrease in the fluorescence emission intensity was observed with increasing salt concentrations. The data suggest that the cysteine residue has a differential degree of exposure at different ionic strengths.

To examine any change in the average distance between cysteine and tryptophans, fluorescence resonance energy transfer measurements were carried out under similar sets of ionic strengths. Interestingly, the emission maximum of tryptophan falls in the range of the excitation maximum for the AN group attached to cysteine. This very aspect of AN group fluorescence was used to see the FRET efficiency of tryptophan as a function of ionic strength of the buffer. There is a gradual increase in the emission intensity of the AN group tagged to cysteine at 455 nm with a simultaneous decrease in emission peak intensity of tryptophan increasing salt concentration until 1 M implying an overall change in the average distance between tryptophans and cysteines (Fig. 4*D*). Such decrease in average distance between tryptophans and cysteines in the HABP1 trimer indicates the conformational changes associated with the molecule upon structural compaction.

Evidence for Salt-mediated Structural Compactness of HABP1 by Limited Proteolysis—The factors determining the vulnerability for proteolysis of a protein by protease depends on the conformational parameters such as accessibility, segmental motion structural compactness, and protrusions. Due to this reason, limited proteolysis has been effectively used to monitor protein surface regions and the solution conformation of the molecule (31). The proteolytic susceptibility of HABP1 to trypsin at 0, 150, and 1 M of salt concentration was analyzed. To compensate any loss of trypsin activity due to increasing ionic strength, enzyme concentration was increased in the same ratio of its decrease as reported earlier (26). There are 21 lysine and arginine residues spread all over the HABP1 molecule, and hence an extensive proteolysis is expected resulting in a number of smaller peptide fragments if the protein exists in an expanded conformation. Indeed, at low salt concentrations, where HABP1 seems to exist in an ensemble of expanded conformations, a number of smaller peptide fragments generated as is evident from the peaks corresponding to lower molecular size on the chromatographic profile of limited trypsin digestion in the absence of salt (Fig. 5). However, at higher salt concentrations (0.15 and 1 M), HABP1 seems relatively resistant toward tryptic digestion compared with that in the absence of salt, as is apparent from the appearance of undigested fractions at 150 mM and beyond. In addition, the peptide fragment of larger size is also detected. Thus, it is logical to conclude that the increased ionic strength leads to inaccessibility of the sites susceptible for protease attack in HABP1, presumably due to enhanced compactness of structure.

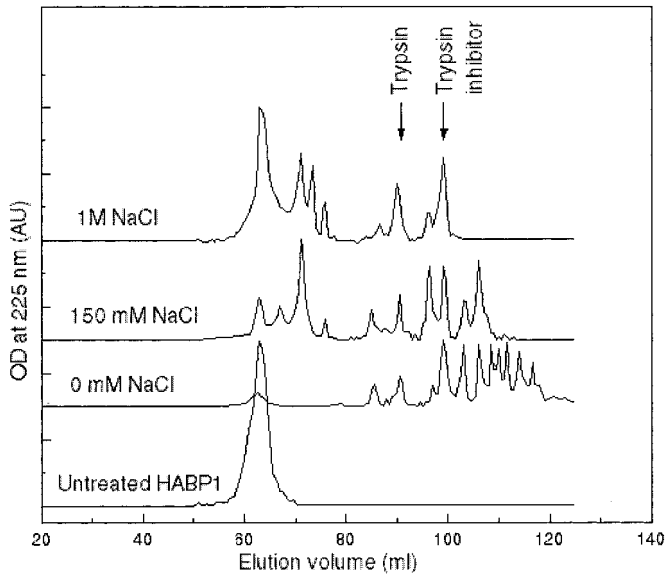

FIG. 5. **Change in protease susceptibility of HABP1 with increasing ionic strength.** HABP1 (1 μM) in 10 mM sodium phosphate buffer was treated with different amounts of NaCl and subjected to limited proteolysis with trypsin as described under "Experimental Procedures." The trypsin digestions were stopped by adding 1:2 (w/w) of soybean trypsin inhibitor and injected on Sephacryl S200 (16/60) prepacked column, and the elution volume was plotted against the absorption at 225 nm. The *arrows* show the mean elution volume of trypsin and soybean trypsin inhibitor run independently on the same column under similar conditions. *y* axis is translated upward for the clarity of data.

Ionic Strength Affects the Ligand Binding of HABP1—In order to examine whether this salt-induced structural transition can regulate the affinity of multifunctional HABP1 toward different ligands, HA, C1q, and DMA, binding assays were performed as a function of increasing salt concentrations as described under "Experimental Procedures." The data demonstrate that there is no binding of HABP1 with HA in absence of salt (Fig. 6*A*); however, the other two ligands, c1q and DMA, show substantial binding under these experimental conditions.

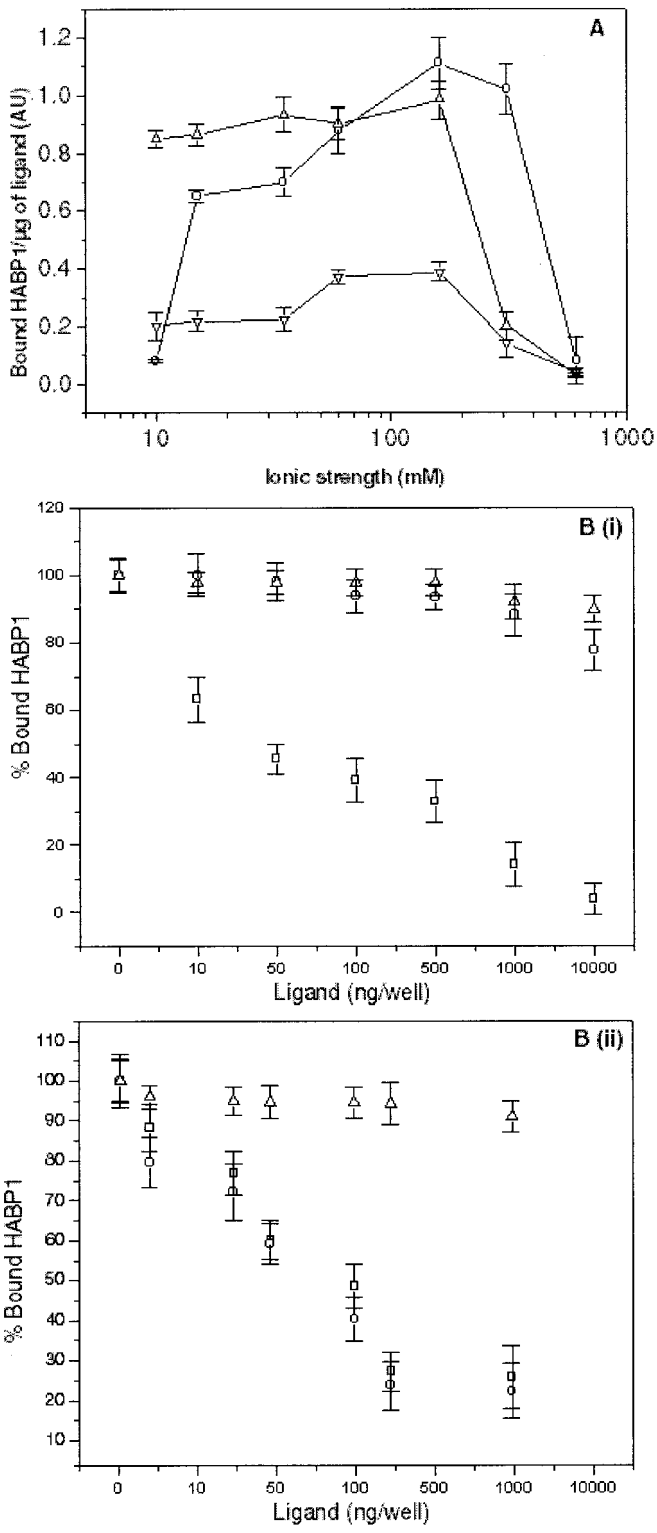

FIG. 6. **Regulation of HABP1 interactions with different ligands by ionic strength.** *A,* differential binding of HABP1 toward different ligands at varying ionic strength. Different ligands of HABP1 (*circle*), HA (*down triangle*), and C1q (*up triangle*) mannosylated albumin were coated in 96-well enzyme-linked immunosorbent assay plate as described under "Experimental Procedures" and incubated with HABP1 in 10 mM phosphate buffer containing different amount of salt and probed with 1:5000 dilution of anti-HABP1 antibodies and developed with 1:10,000 dilution of horseradish peroxidase-conjugated goat anti-rabbit IgG using ABTS as substrate. Bound HABP1 per μg of different ligand was plotted against the ionic strength. *B,* effect of ionic strength on the competition of DMA to HABP1 by other ligands. DMA-coated wells were incubated with biotinylated HABP1, preincubated with varying concentrations of unlabeled HA (*circle*), DMA (*square*), and C1q (*triangle*) in the presence of 10 mM (*i*) and 300 mM (*ii*) of NaCl, and bound HABP1 was detected. Blank wells were coated with buffer alone and were subtracted from the sample wells. Percentage of bound HABP1 was plotted against increasing concentration of ligands. The standard deviation ($n = 3$) is shown as *error bars* on each data point.

There is a gradual increase in HA binding with increasing salt concentrations with maximum binding at around 150 mM NaCl, although such significant changes with the other two ligands were not observed. Beyond 150 mM salt concentrations, a gradual decrease in the binding was observed, which abolished completely above 600 mM ionic strength with all the ligands. Thus, a threshold amount of salt is needed for optimum HA-HABP1 interaction; however, the same is not the case with other two ligands. At higher salt concentrations, the binding is abolished due to various factors including hydrophobic as well as electrostatic interactions, which seem important regulators for the affinity of HABP1, as is the case with several other HA-binding proteins. When DMA-coated wells were assayed with biotinylated HABP1 preincubated with increasing concentrations of unlabeled DMA, HA, or C1q at two extremes of salt concentration, it was observed that at 10 mM of NaCl neither HA nor C1q inhibited HABP1 binding to DMA (Fig. 6*B, i*). However, at higher salt concentrations the inhibition was observed in a dose-dependent manner with HA only (Fig. 6*B, ii*). Preincubation with C1q did not affect the HABP1 binding to DMA, suggesting the fact that C1q and DMA/HA-binding sites on HABP1 are exclusive, and they seems to behave independently. The data at two extremes of salt suggest that DMA and HA may share an overlapping binding site on HABP1; however, their modes of binding are different. Furthermore it is clear from these studies that a minimum three-dimensional rigid structure is needed for any optimum HA-HABP1 interactions, which is not the case with the other two ligands.

DISCUSSION

Recently we have reported that HABP1, a multifunctional protein, exists in different oligomeric forms under various *in vitro* conditions in solution, although the molecule is predominantly trimeric in anaerobic conditions at 150 mM salt concentration (18). HABP1, having an HA-binding motif (Lys^{119}–Lys^{128}), is reported to bind with HA with a K_d of 1.1×10^{-9}, with C1q through the first 24 residues on the NH_2 terminus with a nanomolar dissociation constant (13), and with clustered mannose (29). We were interested in probing its structural behavior under different *in vitro* conditions to address some of its intriguing behaviors. Thus, we have examined the structural plasticity of HABP1 under various *in vitro* conditions as a function of ionic strength, and we tried to correlate the inherent structural flexibility with its binding toward different ligands. Here we provide the experimental evidence for structural transitions of HABP1 induced by the ionic environment around the molecule, which has a direct implication on HA binding compared with the other two ligands.

Existence of Molten Globule-like State of Trimeric HABP1 in Low Ionic Environment—It is evident from several independent experiments, using diverse techniques, that HABP1 exists in a highly expanded structure under low ionic strength. The hydrodynamic volume (V_h) of the molecule in the presence of 10 mM of salt at neutral pH is nearly 1.5 times that in presence of 1 M of salt (Fig. 1*B*). Extensive digestion of HABP1 in the absence of salt into smaller fragments by trypsin also suggests the existence of an expanded structure under such conditions where sites for protease attack are highly accessible (31). Circular dichroism profile in the absence of salt shows a minimum at 205 nm which changes to a double minima at ~210 and ~220 nm, typical of $\alpha + \beta$ class of proteins suggesting the

existence of disordered structure of HABP1 under low ionic strength, which changes to more ordered structure with increasing ionic strength. The efficiency of FRET is minimum in the buffers of low ionic strength suggesting the large distance of Cys^{186} from the tryptophans (Fig. 4*D*). Hydrophobic reporter dye, ANS, binding was found maximum in low ionic environment (Fig. 2). This suggests that the expanded structure of HABP1 may be similar to molten globule-like state under low ionic environment, which is in agreement with several recent reports (32). All experimental evidence suggests that at a low ionic environment HABP1 exists in an expanded molten globule-like state, which attains a globular conformation above 50 mM of salt concentrations. Our observations are in agreement with the recent reports (32–35) of salt-mediated disorder-order transition of several other highly acidic proteins similar to HABP1.

Transitions from Expanded to Compact Trimer with Increasing Ionic Strength—The gradual increase in ionic strength (150 mM to 1 M) results in a simultaneous decrease in shape and size of the molecule with increased secondary structural content. It is concluded on the basis of several independent experiments demonstrating the decrease in hydrodynamic volume (V_h), intrinsic tryptophan fluorescence, extrinsic fluorescence emission intensity of anilinonaphthyl group tagged at Cys^{186}, complete abolition of ANS binding above 50 mM salt concentration, and increased FRET efficiency of the molecule. Neutralization of charges on HABP1 by counter ions seems to promote the transition from disordered to ordered structure, which is in agreement with recent reports (34–36).

This global change in the shape of the molecule seems to originate from the different conformations that the molecule adapts under the influence of changes in ionic strength. Our observations of the gradual decrease in the intrinsic as well as extrinsic fluorescence intensities suggest that the salt-induced changes in hydrodynamic volume of the molecule leads to the conformational change of the molecule. A gradual change in tryptophan fluorescence emission intensity results from the gradual inaccessibility of the indole ring to the solvent. This interpretation is strengthened by the fact that iodide, a polar fluorescence quencher, quenches fluorescence emission intensity at much faster rate in the buffer of low ionic strength than that of high ionic strength. Solvent accessibility of cysteine also seems to be affected by the ionic strength of the environment around the molecule, which is consistent with the earlier observations (18) where trimeric HABP1 is shown to dimerize through the only cysteine present in each molecule under oxidative conditions.

Structural Plasticity of HABP1 Regulates Its Binding toward Different Ligands—HABP1 is an acidic protein (pI 4.1) with low intrinsic hydrophobicity and high net charge at neutral pH. The trimeric HABP1 has a charge of −81 at pH 7.2. Most of the negative charges are present on one surface including the inner wall of the propeller-like channel of the molecule (14). This surface charge localization may allow the electrostatic repulsion to take predominance over other interactions in dictating the folding topology and three-dimensional structure. The asymmetric charge distribution along the faces of HABP1 may force the molecule to exist in marginally stable, expanded conformations at 10–25 mM ionic strength (37). This marginally stable expanded conformation attains a compact stable structure at 150–600 mM, which further becomes more compact at higher salt concentration (600 mM to 1 M).

The structural plasticity of HABP1 may play an important role in regulating its binding toward different ligands. Under the conditions of 10 mM ionic strength, where HABP1 exists in a loosely held trimeric structure, it fails to bind HA. However, it shows appreciable binding with other reported ligands/interacting molecules, namely C1q and clustered mannose (Fig. 6*A*). This fact suggests that binding of HABP1 toward different ligands is governed by its structural state. The binding of HABP1 toward HA shows a drastic change from 0 mM of NaCl (no binding) to 20 mM of NaCl (substantial binding), where HABP1 gains structure to some extent. Further increase in HA binding with increasing salt concentration up to 150 mM suggests the improvement of binding due to the better structural fit of the HABP1 for its ligand HA. Other ligands do not show any significant change in binding levels under a similar set of conditions. Salt-induced structural variations of HABP1 affect hyaluronan binding and the binding of two other ligands to loosely held trimeric HABP1 and facilitated interesting insights into the nature of the binding sites on HABP1 for three different ligands. C1q does not show any appreciable inhibition of DMA binding at any ionic strength, although it can bind with the loosely held (at 10 mM) as well as compact (at 300 mM) trimeric HABP1. Our data suggest that C1q, which binds at NH_2-terminal region of HABP1, remains unaffected with DMA binding. It is apparent that C1q-binding site on HABP1 is independent of DMA/HA-binding sites, and its nature of binding is also different. Our data on the competitive inhibition of HABP1 binding to DMA by HA only at higher ionic strength where HA can bind to HABP1 suggests that HA and DMA share an overlapping binding site on HABP1. However, at low ionic strength, where HA does not bind to HABP1, it fails to inhibit the HABP1-DMA binding, implying that the nature of binding of HA and DMA are different. Thus, it appears logical to argue that a minimum rigid three-dimensional structure apart from the presence of BX_7B (where B stands for any basic and *X* for any non-acidic amino acid residues) motif is essential for any relevant HA-HABP1 affinity, which is recently proposed by Day and Prestwich (2). The salt-induced effects on the structure and stability of HABP1 are attributed to the binding of counter ions, resulting in minimization of intramolecular electrostatic repulsion. This leads to increased stability and greater compactness in the structure, as observed. Consequently, localized electrostatic repulsion is present at neutral pH in HABP1, probably contributing to expanded molten globule-like structure and its marginal stability.

The transitions from loosely held trimeric structure to compact ordered structure might be linked with one of its reported functions as a molecular chaperon. HABP1 is known to regulate the kinase activity of almost all isoforms of protein kinase C at 50 mM ionic strength under reducing conditions without being their substrate like a molecular chaperon (38–39). In this context these structural transitions are important because of the fact that the accessible hydrophobic surface is the key element for chaperon-like action (40). It is important to mention that our observation demonstrates that the hydrophobic surface remains accessible at 50 mM ionic strength supporting its molecular chaperon-like activity demonstrated with protein kinase C (39). These accessible surfaces can be perturbed by the change in the ionic strength in the microenvironment of the molecule (41). Finally, it may be noted that HABP1 may belong to the group of eukaryote proteins, which remain only partially structured under physiological conditions and execute numerous functions consistent with the physico-chemical microenvironment of the molecule.

Acknowledgment—We thank Prof. Avadhesh Surolia, Indian Institute of Sciences, Bangalore, India, for his critical comments on manuscript.

REFERENCES

1. Lee, J. Y., and Spicer, A. P. (2000) *Curr. Opin. Cell Biol.* **12,** 581–586
2. Day, A. J., and Prestwich, G. D. (2002) *J. Biol. Chem.* **277,** 4585–4588

3. Turley, E. A., Bourguignon, L., and Noble, P. W. (2002) *J. Biol. Chem.* **277,** 4589–4592
4. Toole, B. P., Wright, T. N., and Tammi, M. I. (2002) *J. Biol. Chem.* **277,** 4593–4596
5. Fraser, J. R. E., and Laurent, T. C. (1996) in *Extracellular Matrix, Molecular Components and Interactions* (Comper, W. D., ed) pp. 141–199, Vol. 2, Harwood Academic Publishers, Amsterdam
6. D'Souza, M., and Datta, K. (1985) *Biochem. Int.* **10,** 43–51
7. Deb, T. B., and Datta, K. (1996) *J. Biol. Chem.* **269,** 2206–2212
8. Gupta, S., Babu, B. R., and Datta, K. (1991) *Eur. J. Cell Biol.* **56,** 58–67
9. Gupta, S., and Datta, K. (1991) *Exp. Cell Res.* **195,** 386–394
10. Ranganathan, S., Ganguly, A. K., and Datta, K. (1994) *Mol. Reprod. Dev.* **38,** 69–76
11. Ranganathan, S., Bharadwaj, A., and Datta, K. (1995) *Cell. Mol. Biol. Res.* **41,** 467–476
12. Krainer, A. R., Mayeda, A., Kozak, D., and Binns, G. (1991) *Cell* **66,** 383–394
13. Ghebrehiwet, B., Lim, B. L., Peerschke, E. I. B., Willis, C. A., and Reid, K. B. M. (1994) *J. Exp. Med.* **179,** 1809–1821
14. Jiang, J., Zhang, Y., Krainer, A. R., and Xu, R. M. (1999) *Proc. Natl. Acad. Sci. U. S. A.* **96,** 3572–3577
15. Soltys, B. J., Kang, D., and Gupta, R. S. (2000) *Histochem. Cell Biol.* **114,** 245–255
16. Brokstad, K. A., Kalland, K. H., Russell, W. C., and Matthews, D. A. (2001) *Biochem. Biophys. Res. Commun.* **281,** 1161–1169
17. Majumdar, M., Meenakshi, J., Goswami, S., and Datta, K. (2002) *Biochem. Biophys. Res. Commun.* **291,** 829–837
18. Jha, B. K., Salunke, D. M., and Datta, K. (2002) *Eur. J. Biochem.* **269,** 298–306
19. Records, M. T., Jr., Zhang, W., and Anderson, C. F. (1998) *Adv. Protein Chem.* **51,** 281–353
20. Gill, S. C., and Hippel V. H. (1989) *Anal. Biochem.* **6,** 319–326
21. Siegel, L. M., and Monty, K. J. (1966) *Biochim. Biophys. Acta* **112,** 346–362
22. Denning, P. D., Uversky, V., Patel, S. S., and Fink, A. L. (2002) *J. Biol. Chem.* **277,** 33447–33455
23. Ahmad, A., Akhtar, M. S., and Bhakuni, V. (2001) *Biochemistry* **40,** 1945–1955
24. Yoshimura, T. (1993) *Methods Enzymol.* **221,** 72–77
25. Ohyashiki, T., Sekine, T., and Kanaoka, Y. (1974) *Biochim. Biophys. Acta* **351,** 214–216
26. Strzelecka-Golaszewska, H., Wozniak, A., Hult, T., and Lindberg, U. (1996) *Biochem. J.* **316,** 713–721
27. Khoda, D., Morton, C. J., Parkar, A. A., Hatanaka, H., Inagaki, F. M., Campbell, I. D., and Day, A. J. (1996) *Cell* **86,** 767–775
28. Parkar, A. A., Kahmann, J. D., Howat, S. L. T., Bayliss, M. T., and Day, A. J. (1998) *FEBS Lett.* **428,** 171–176
29. Kumar, R., Roychoudhary, N., Salunke, D. M., and Datta, K. (2001) *J. Biosci.* **26,** 325–332
30. Eftink, M. R., and Ghiron, C. A. (1981) *Anal. Biochem.* **114,** 199–227
31. Hubbard, S. J (1998) *Biochim. Biophys. Acta* **1382,** 191–206
32. Uversky, V. N. (2002) *Protein Sci.* **11,** 739–756
33. Xie, D., Bhakuni, V., and Freire, E. (1993) *J. Mol. Biol.* **232,** 5–8
34. Sakurai, K., Oobatake, M., and Goto, Y. (2001) *Protein Sci.* **10,** 2325–2335
35. Jekow, P., Behlke, J., Tichelaar, W., Lurz, R., Regalla, M., Hinrichs, W., and Tavares, P. (1999) *Eur. J. Biochem.* **264,** 724–735
36. Nishimura, C., Uversky, V. N., and Fink, A. L. (2001) *Biochemistry* **40,** 2113–2128
37. Akhtar, M. S., Ahmad, A., and Bhakuni, V. (2002) *Biochemistry* **41,** 7142–7149
38. Sortz, P., Hausser, A., Link, G., Dedio, J., Ghebrehiwet, B., Pfizenmaier, K., and Johannes, F. J. (2000) *J. Biol. Chem.* **275,** 24601–24607
39. Flores, M. R., Huerta, E. R., Aguilar, H. G., Hernandez, G. M., Islas, S., Mendoza, V., Castaneda, V. P., Mariscal, L. G., and Casillas, F. L. (2002) *J. Biol. Chem.* **277,** 5247–5255
40. Horowitz, P. M., Hua, S., and Gibbons, D. L. (1995) *J. Biol. Chem.* **270,** 1535–1542
41. Sheluho, D., and Ackerman, S. H. (2001) *J. Biol. Chem.* **276,** 39945–39949